Physics Letters A 380 (2016) 2892–2896

Contents lists available at ScienceDirect

Physics Letters A

www.elsevier.com/locate/pla

Observation of parametric X-ray radiation in an anomalous diffraction region

V.I. Alexeyev [a,b], A.N. Eliseyev [a,b], E. Irribarra [c], I.A. Kishin [a,b], A.S. Kubankin [a,b,*], R.M. Nazhmudinov [a,b]

[a] P.N. Lebedev Physical Institute RAS, 53 Leninskiy prospect, Moscow, Russia
[b] Belgorod National Research University, 85 Pobedy st., Belgorod, Russia
[c] Escuela Politécnica Nacional, Ladrón de Guevara E11-253, Quito, Ecuador

ARTICLE INFO

Article history:
Received 19 May 2016
Received in revised form 28 June 2016
Accepted 28 June 2016
Available online 9 July 2016
Communicated by V.A. Markel

Keywords:
Parametric X-ray radiation
Relativistic particles
X-ray diffraction
Virtual photons

ABSTRACT

A new possibility to expand the energy region of diffraction processes based on the interaction of relativistic charged particles with crystalline structures is presented. Diffracted photons related to parametric X-ray radiation produced by relativistic electrons are detected below the low energy threshold for the X-ray diffraction mechanism in crystalline structures for the first time. The measurements were performed during the interaction of 7 MeV electrons with a textured polycrystalline tungsten foil and a highly oriented pyrolytic graphite crystal. The experiment results are in good agreement with a developed model based on the PXR kinematical theory. The developed experimental approach can be applied to separate the contributions of real and virtual photons to the total diffracted radiation generated during the interaction of relativistic charged particles with crystalline targets.

1. Introduction

Nowadays diffraction processes for electromagnetic waves and particles are well studied [1,2]. A third group of diffraction processes occurs during coherent scattering of the charged particles Coulomb field (field of virtual photons) on atomic structures [3]. Quasi-monochromatic X-ray beams are generated during such interaction and their characteristics depend on the parameters of both the atomic structure and the incidence particle beam. Such mechanism of radiation generation is called “Parametric X-ray radiation” (PXR) [4]. Besides, this mechanism is the coherent component of the polarization bremsstrahlung [5,6]. PXR can be used to produce monochromatic X-ray beams [7], to control the characteristics of charged particles beams [8] and to determine the atomic structure parameters [9,10].

PXR is concentrated in a hollow cone around the Bragg direction. The typical angular size of PXR distribution is

$$\pm\sqrt{\gamma^{-2}+\omega_0^2/\omega^2}$$

where γ – Lorenz-factor of the relativistic electron, ω_0 – plasma frequency of the atoms and ω – energy of emitted photons. The PXR spectrum consists of a set of peaks, which positions can be approximately described by the Bragg law for free X-rays diffraction.

The diffraction processes of free X-rays and of virtual photons have similar spectral and angular characteristics. The differences between the diffraction of virtual and real photons on atomic structures arise because of two well-known important factors, whose influence is reflected in the spectral–angular distribution of detected photons. The first consists in the velocities difference of the charged particles (virtual photons source) and free X-rays [11,12]. Because the energy of PXR photons is proportional to the particle velocity, the difference between velocities produces a shift of the PXR peaks position in the spectrum towards the soft energies by a coefficient proportional to c/V (c and V are the velocities of light and charged particles respectively); this factor becomes negligible for relativistic particles when V approaches c. The second factor is related to the initial angular distribution of real and virtual photons [13,14].

The contribution of the real photons diffraction mechanism to the total radiation yield can be substantial in a wide spectral range of emitted photons. The diffracted bremsstrahlung contribution (DB) dominates in the spectral range $\omega > \gamma\omega_0$ [14], while the diffracted transition radiation (DTR) contribution dominates in the spectral range $\omega < \gamma\omega_0$ [13,15,16]. The separation of the DTR, DB

* Corresponding author.
E-mail addresses: vial@x4u.lebedev.ru (V.I. Alexeyev), elisseev@pluton.lpi.troitsk.ru (A.N. Eliseyev), esteban.irribarra@epn.edu.ec (E. Irribarra), ivan.kishin@mail.ru (I.A. Kishin), kubankin@bsu.edu.ru (A.S. Kubankin), fizeg@bk.ru (R.M. Nazhmudinov).

http://dx.doi.org/10.1016/j.physleta.2016.06.055
0375-9601/

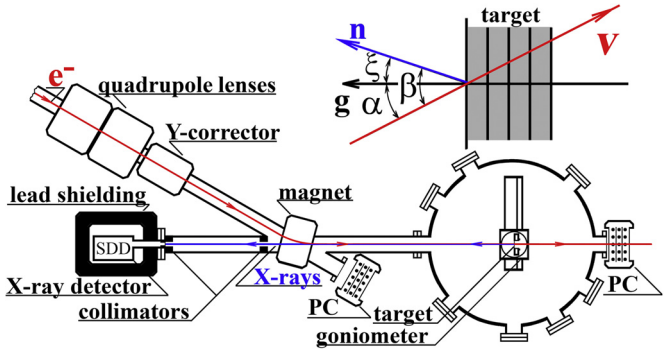

Fig. 1. The experimental setup geometry. $\boldsymbol{n}$ – unit vector in the direction of the radiation propagation, $\boldsymbol{V}$ – incident electron velocity vector, $\mathbf{g}$ – reciprocal lattice vector.

and PXR yields is a difficult task because the typical angular and spectral distributions of these mechanisms are close, especially in conditions when the angle of electron beam multiple scattering on the effective trajectory length of the electrons in the target is comparable with the typical size of PXR angular distribution $\sqrt{\gamma^{-2}+\omega_0^2/\omega^2}$.

This work presents the first observation of a diffraction process in a region, which is below the lowest diffraction threshold for X-rays. Here and after this region will be called "anomalous" diffraction region. The results can be applied to separate the contributions of real and virtual photons to the total diffraction yield produced during the interaction of charged particles with atomic structures. It should be mentioned that the experimental separation of the contributions is a classical task difficult to achieve, which was mainly solved theoretically. For this reason, in a number of experimental works devoted to PXR it was assumed that the registered signal had a predominant PXR contribution or the total yield was presented as a sum of different radiation mechanisms (PXR, diffracted bremsstrahlung, diffracted transition radiation) but an experimental separation of the contributions was not achieved [17–23].

The experiment was performed in the backward geometry where the detected radiation propagates in the opposite direction with respect to the incident electrons. A theoretical model based on the PXR kinematical theory [24] was developed in the work to describe the PXR in the anomalous energy region. The relativistic system of units $\hbar = c = 1$ is used.

2. Experimental setup

The experimental setup schematically presented in Fig. 1 was developed in the department of High Energy Physics of the P.N. Lebedev Physical Institute of RAS (described in detail in [23]). The setup used a 7 MeV energy electron beam produced by a microtron. The beam is transported to the target using a magneto optical system consisting of three bending magnets (only the last magnet is presented in Fig. 1), two pairs of quadrupole lenses and a Y-corrector. The beam intensity and position were controlled by a Faraday cup and two gas proportional chambers (PC) respectively. The system was specially designed to perform measurements in conditions of low radiation background.

The initial beam angular divergence at the target location point was less than 5 mrad and the beam diameter was less than 3 mm. The 20 μm thickness tungsten polycrystalline foil used in [23] and a 1 mm thickness highly oriented pyrolytic graphite (HOPG) crystal were used as targets. The mosaic angles (FWHM) of the targets are: 5.44° for the tungsten (200) plane, which has a predominant orientation parallel the target surface; and 0.4° for the HOPG. The orientation of the targets was remotely controlled by a goniometer, which has three degrees of freedom. The accuracy of the target rotation relative to the electron beam axis in the horizontal and vertical planes was 0.01 degrees. The goniometer also allowed one to take the target off the electron beam to control and adjust the position and divergence of the beam without the influence of the target on the beam.

The radiation generated during the interaction of the electrons with the target was collimated in a $1.5 \cdot 10^{-7}$ sr. solid angle and registered by the detector (Amptek X-123 FAST SDD). The detector was calibrated under the experimental conditions using characteristic X-ray lines excited by the electron beam in different elements (Ni, Cu, Si, W, Ti). The peaks energy coincided with the values of [25] within ±0.1% for all lines. The calibration allows one to define the energy of the PXR peaks with high accuracy, sufficient for the results interpretation.

Under the mentioned conditions, the detector registered the radiation only from the target and its holder, made of PMMA (methyl methacrylate). The thicknesses of the target and holder were chosen for suppression of the radiation generated in the backward geometry during the interaction of the beam with the proportional chamber in the 1–6 keV energy range where the PXR signal was expected. The geometry used allowed one to measure a clear PXR signal.

3. Theory

In accordance with Fig. 1 the geometry of the electron beam interaction with the target can be determined by three vectors and the corresponding angles: the orientation angle α, the observation angle β and the diffraction angle ξ. The energy of PXR photons is determined by all three angles, whereas according to the Bragg law the energy of X-ray diffraction (XRD) depends only on ξ. The PXR and XRD energies can be presented as follows [26,27]:

$$\omega^{PXR} = \frac{-\mathbf{g}\cdot\boldsymbol{V}}{1-\sqrt{\varepsilon}\boldsymbol{n}\cdot\boldsymbol{V}} \approx \lim_{\substack{V\to 1\\ \varepsilon\to 1}} \frac{-\mathbf{g}\cdot\boldsymbol{V}}{1-\sqrt{\varepsilon}\boldsymbol{n}\cdot\boldsymbol{V}} = \frac{g\cos(\alpha)}{2\cos^2(\frac{\beta}{2})} \tag{1a}$$

$$\omega^{XRD} = \frac{g^2}{2\,\boldsymbol{n}\cdot\mathbf{g}} = \frac{g}{2\cos(\xi)}. \tag{1b}$$

In accordance with (1b), the diffracted real photons have a low energy threshold at the diffraction angle $\xi = 0$ while the PXR energy can be lower if $\beta = 0$ and $\alpha \neq 0$. Therefore, the backward geometry allows one to observe the PXR in the anomalous diffraction region. This effect clearly shows the difference between diffraction processes of virtual and real photons.

According to the kinematical description of PXR (see [4,24, 28]), the spectral–angular distribution can be presented in a vector form:

$$\omega\frac{d^3N}{dtd\omega d\Omega} = \frac{e^2\omega_g^4}{2\pi}\frac{(\boldsymbol{V}\cdot\boldsymbol{e}_{10})^2+(\boldsymbol{V}\cdot\mathbf{e}_{20})^2(\mathbf{e}_{20}\cdot\mathbf{e}_{2g})^2}{(g^2+2\sqrt{\varepsilon}\omega\boldsymbol{n}\cdot\mathbf{g})^2} \times\delta\left[\omega(1-\sqrt{\varepsilon}\boldsymbol{n}\cdot\boldsymbol{V})+\mathbf{g}\cdot\boldsymbol{V}\right], \tag{2}$$

where $\omega_g^2 = \omega_p^2(F(g)/Z)(S(\mathbf{g})/N_0)\exp(-g^2u_T^2)$, $F(g)$ is the form-factor of an atom, Z is the atomic number, $S(\mathbf{g})$ is the structure factor of an elementary cell containing N_0 atoms, u_T is the mean-square amplitude of thermal vibrations of atoms, the unit polarization vectors $\boldsymbol{e}_{i0}$ and $\boldsymbol{e}_{ig}$ correspond to the primary and diffracted fields respectively (index $i = 1$ corresponds to the S polarization). The angular variables presented in Fig. 2 are helpful to describe the PXR spectral–angular distribution considering: the influence of multiple scattering of the electron beam in the target ($\boldsymbol{\Psi} = \boldsymbol{\Psi}_\parallel + \boldsymbol{\Psi}_\perp$), the finite size of the detector ($\boldsymbol{\Theta} = \boldsymbol{\Theta}_\parallel + \boldsymbol{\Theta}_\perp$) and the possible irregularity of the target atomic structure ($\boldsymbol{\eta} = \boldsymbol{\eta}_\parallel + \boldsymbol{\eta}_\perp$). The unit vectors $\boldsymbol{e}_{\rm inc}$ and $\boldsymbol{e}_{\rm sp}$ correspond to the directions of the